Iraqi Journal of Physics, 2024 *Vol. 22, No. 3, PP. 50-59*
https://doi.org/10.30723/ijp.v22i3.1269 *P-ISSN: 2070-4003*
E-ISSN: 2664-5548

Analysis of the Double Head Streamer Discharge Simulation under Different Pressures

Maha F. Abdulameer[1a*] and Thamir H. Khalaf [1b]
[1] *Department of physics, College of science, University of Baghdad, Baghdad, Iraq*
[b]E-mail: thamir.Khalaf@sc.uobaghdad.edu.iq
[a*]Corresponding author: maha.f@sc.uobaghdad.edu.iq

Abstract

In this research, the dynamics of double-head streamer discharge initiation, propagation, interaction and breakdown in the air under different pressure values were presented. The double-head streamer discharge dynamics were analysed within a plane-to-plane electrode configuration. That was done through many aspects proposed, such as electron density, electric field**,** space charge density and streamer propagation speed. The simulation performed using 'COMSOL Multiphysics' is based on the finite element method and was carried out with the fluid model. The fluid model describes the movement of particle concentrations using partial differential equations (PDEs) together with Poisson's equation; Poisson's equation and charge concentrations determine the electric field distribution in space. According to the results, as the pressure increased from (1, 2 and 3atm), the evolution time of the streamer increased from (0.563 to16.29ns) with the same breakdown voltage of 19kV. This means that the double-head streamer discharge developed faster with the decrease in pressure.

Article Info.

Keywords:
Streamer Discharge, Fluid Model, Finite Element Method, Plane-to-plane Air Gap, COMSOL Multiphysics.

Article history:
Received: Apr. 23, 2024
Revised: May, 22, 2024
Accepted: May,24, 2024
Published: Sep. 01, 2024

1. Introduction

Typically, atmospheric air is widely used as an insulating medium in many overhead power lines and electrical equipment because it has a breakdown strength of 30 kV/cm [1]. In air with normal pressure, discharges typically take the shape of thin plasma filaments, sometimes called streamers [2]. The formation of a discharge requires two conditions: first, a sufficiently high electric field should be present in a sufficiently large region. Second, free electrons should be present in this region. If no or few of these electrons are present, the discharge may form with a significant delay or not at all [3]. One can divide streamers into two groups: positive and negative. Negative streamers grow in the opposite way from positive streamers, which spread along the same direction of the electric field [3]. When negative and positive streamers are combined, double-headed streamers are produced, which propagate simultaneously in two directions [4]. Generally, double-head streamer discharges have four physically dominant regions: (i) A 'non-ionized outer area' where the Poisson equation must be solved, (ii) an electron avalanche zone, where electron seeds form multiple electron avalanches, the electron avalanche enters the streamer domain when space charge effects become important [5], (iii) The moving negative and positive streamer heads' active space charge layer creates a non-zero net charge where ionization happens quickly and the field is the strongest, and (iv) Equal-charged ionized channels; which represent a quasi-neutral plasma conductor [5, 6].

Streamer physics may be studied, and experimental results can be explained with

using numerical simulations [7]. Models and simulation methods for electrical discharges have been developed for almost fifty years. Several models have been created to investigate the spread of streamers; these models fall into four categories: hybrid, kinetic, fluid, and particle models [8]. At standard temperature and pressure, streamers in air contain at least of the order of 10^7 electrons when they emerge from avalanches through the build-up of a space charge layer [9, 10]; it is very difficult to follow this growing number of electrons individually inside the streamer discharge during the development [11]. For this reason, fluid models are used for most streamer simulations [12]. The fluid model of double-head streamer discharges in this research comprises a set of time-dependent highly non-linear partial differential equations (PDEs) that describe charge transport by diffusion and drift under the effect of electric field incorporating different reactions (e.g., electron attachment, ionization, recombination etc. [13]). In this research, the effect of different pressure values (1atm, 2atm and 3atm) on the initiation and breakdown times, electron density, propagation velocity, space charge density, and the electric field of the double-head streamer discharge was studied.

2. Model of Simulation

2.1. Mathematical Model

The continuity equations, which account for electron mobility, generation, and loss, positive and negative ions, and space-charge growth, are the simplest fluid model equations for gaseous discharges. This set of equations is combined with Poisson's equation to account for space-charge-induced electric field modulation [14]. The finite element technique solves the three-species drift-diffusion model equations:

$$\frac{\partial n_e}{\partial t} + \nabla . (n_e \mu_e E - D_e \nabla n_e) = \alpha\, n_e |\mu_e E| - \eta\, n_e |\mu_e E| - \beta_{ep} n_e n_p \quad (\mathbf{1})$$

$$\frac{\partial n_p}{\partial t} + \nabla . (n_p \mu_p E - D_p \nabla n_p) = \alpha\, n_e |\mu_e E| - \beta_{ep} n_e n_p - \beta_{pn} n_p n_n \quad (\mathbf{2})$$

$$\frac{\partial n_n}{\partial t} + \nabla . (n_n \mu_n E - D_n \nabla n_n) = \eta\, n_e |\mu_e E| - \beta_{pn} n_p n_n \quad (\mathbf{3})$$

These equations account for charged species drift under the electric field. The equations' subscripts e, p, and n indicate electrons, positive and negative ions. Poisson's equation for electric potential (V) determines electric field. From the solution of this equation, the electric field values are obtained [15-17]:

$$\nabla (-\varepsilon_0 \varepsilon_r \nabla V) = e\,(n_p - n_e - n_n) \quad (\mathbf{4})$$

where: ε_0 : Vacuum Permittivity ($\varepsilon_0 = 8.85 \times 10^{-12}$ F/m),ε_r: Relative permittivity ($\varepsilon_r = 1$ for air).

2.1. Geometric Model

To simulate 'the actual application' environment of an insulating medium (air), two plane electrodes separated by a distance d in the air are considered. Two-dimensional axisymmetric (r, z dependent) is often used in the case of streamer discharge in atmospheric pressure air. Fig.1 shows the cross-section of geometry; the domain is cylindrically symmetric and is given by the rectangle [0, r] × [0, z] cm^2. The anode and cathode are perpendicular to the axisymmetric (r = 0). The vertical red

broken line that runs from top to bottom is the axis of symmetry. The upper boundary is the plane electrode, which is set as 'the cathode' and is grounded. The lower boundary

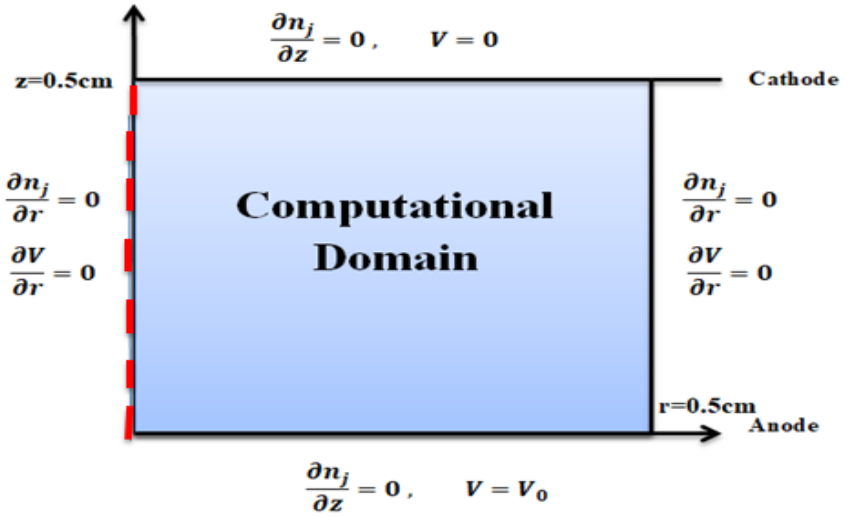

is the planar electrode, which is set as 'the anode' and is subjected to a positive DC high voltage. The remaining boundaries are 'an open boundary'.

Figure 1: The cross section of the geometric model used in this simulation.

2.3. Initial and Boundary Condition

To avoid the long formation stages of streamers and, therefore, initiating a streamer discharge directly, a quasi-neutral plasma spot containing an equal number of charge carriers [18] (electrons and positive ions of Gaussian shape) can be introduced in the middle of the gap to start the double head streamer [19]. These seeds are very important in uniform fields [20]. Charge carriers increase the electron density in the high-field area [21]. The seed plasma had the shape [19]:

$$n_e(r,z)|_{t=0} = n_p(r,z)|_{t=0} = n_{bk} + n_0 \exp\left[-\left(\frac{z - z_0}{s_z}\right)^2 - \left(\frac{r - r_0}{s_r}\right)^2\right] \quad (5)$$

This seed has a length (s_z) of 2 mm and a width (s_r) of 2 mm [21]. A peak density n_0 of 10^{14} cm^{-3} [22], and n_{bk} denotes a uniform background electron density with values 10^8 cm^{-3} [22]. The boundary conditions for each of the Partial Differential Equations (PDEs) are listed in Fig. 1. The variables used in the simulations of double head-streamer discharge in the air are shown in Table 1.

Table 1: Variables used in the simulations of the double-head streamer discharge in the air.

Properties	unit	Functions
α	cm^{-1}	$3500 \exp(-1.65 \times 10^5 \ E^{-1})$ The ionization coefficient [23].
η	cm^{-1}	$15 \exp(-2.5 \times 10^4 \ E^{-1}$ The attachment coefficient [23].
β_{ep}	$cm^3.s^{-1}$	Electron-ion recombination 2×10^{-7} [24].
β_{np}	$cm^3.s^{-1}$	Ion-ion recombination 2×10^{-7} [24].
DeL	$cm^2.s^{-1}$	1800 The longitudinal direction diffusion coefficients [23].
DeT	$cm^2.s^{-1}$	2190 The transverse direction diffusion coefficients [23].
μ_e	$cm^2.V^{-1}.s^{-1}$	The mobility of electron $2.9 \times 10^5 / P$ [25].
μ_i	$cm^2.V^{-1}.s^{-1}$	The mobility of ion $2.6 \times 10^3 / P$ [25].

2.4. Mesh Generation

The fluid model applied to streamers needs to have a very small mesh to capture the steep gradients; it also needs to cover a vast area to consider application-relevant geometry [26]. A narrow, curved, charged layer is present at the front of a streamer. To continue developing the streamer, this charged layer must be resolved as best as possible because it is responsible for producing the electric field that is needed. A small mesh size for the computational grid is required due to the thinness of the charged layer [27]. Fig. 2a shows the simulation region divided into several fine grids, with the most suitable grid structure applied close to the symmetry line. In areas distant from the symmetry axis, a coarse network structure was employed, which significantly increased

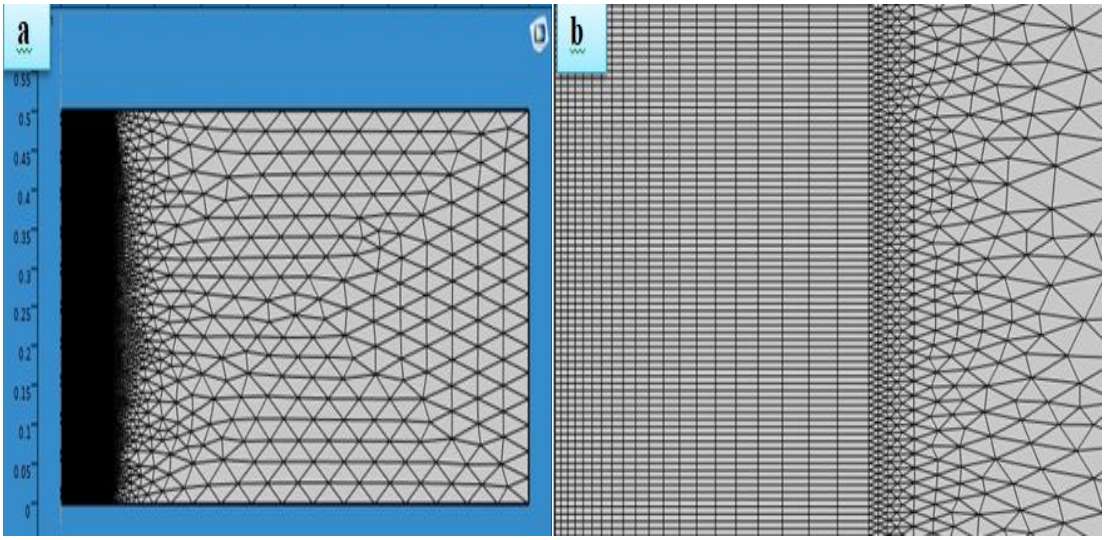

the precision of numerical computations [28]. The mesh zoom and the precision of some mesh entanglement in this model are shown in Fig. 2b.

Figure 2: Two-dimensional axisymmetric diagrams (a) mesh map area (b) zooms of the mesh.

3. Results and Discussion

The results revealed the effect of pressure values on the initiation and breakdown times, electrons density, propagation velocity, space charge density, and the strength of electric field of the double-head streamer discharge.

3.1. The Electrons Concentration

Fig. 3 shows the electron density for the initiation stage of the double-head streamer discharge for the various pressure values. From the figure, a short inception stage can be seen close to the middle of the air gap; the applied voltage created an electric field that caused the seed of positive ions and electrons to be absorbed into the middle of the gap, leaving behind positive and negative space charges which initiated the double-head streamer discharge. For the pressures 1atm, 2atm and 3atm, the double-head streamer was initiated at 0.563, 1.1056, and 1.629 ns, respectively.

Fig. 4 shows the electron density for the propagation stage of the double head streamer discharge in air for the different values of pressure, this stage takes most of the time. For the pressure 1atm, the double head streamer propagated in (1.126 to 3.941) ns and the electron density at the positive streamer head 1.02×10^{14} cm^{-3} as opposed 1.735×10^{13} cm^{-3} for the negative streamer head. When the pressure increased to 2atm; the double head streamer propagated in (2.213 to 7.7455) ns and the electron density at the positive streamer head 1.08×10^{14} cm^{-3} as opposed to 1.95×10^{13} cm^{-3} for the negative

streamer head. With more increased in pressure to 3atm; the double head streamer propagated in (3.258 to 13.032) ns and the electron density at the positive streamer head 1.08×10^{14} cm^{-3} as opposed to 2.45×10^{13} cm^{-3} for the negative streamer head.

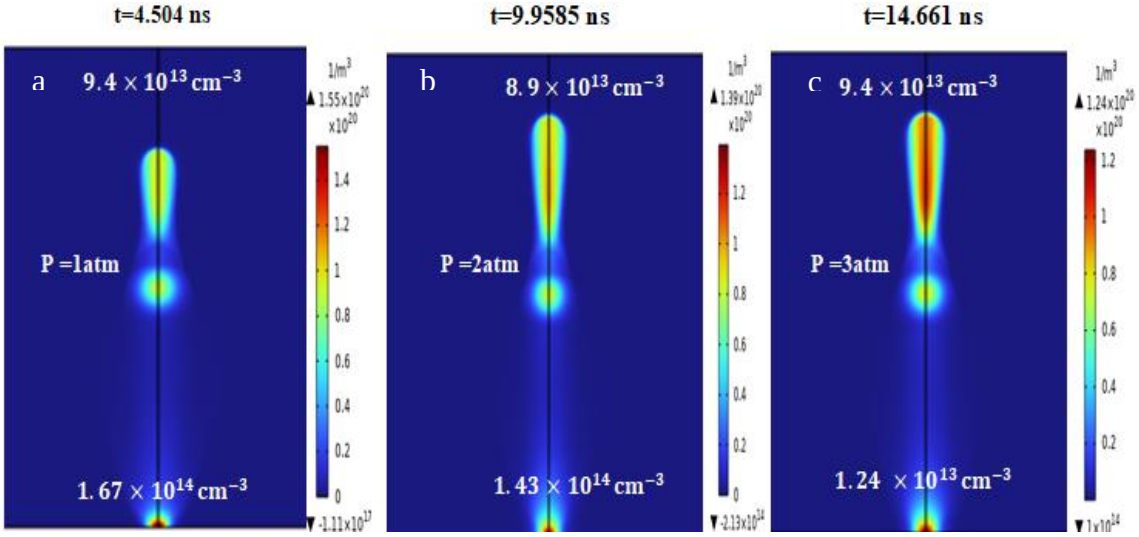

Figure 3: Two-dimensional surface plots of the electron density (the inception stage) of a double-head streamer discharge extending between plane-to-plane electrodes.

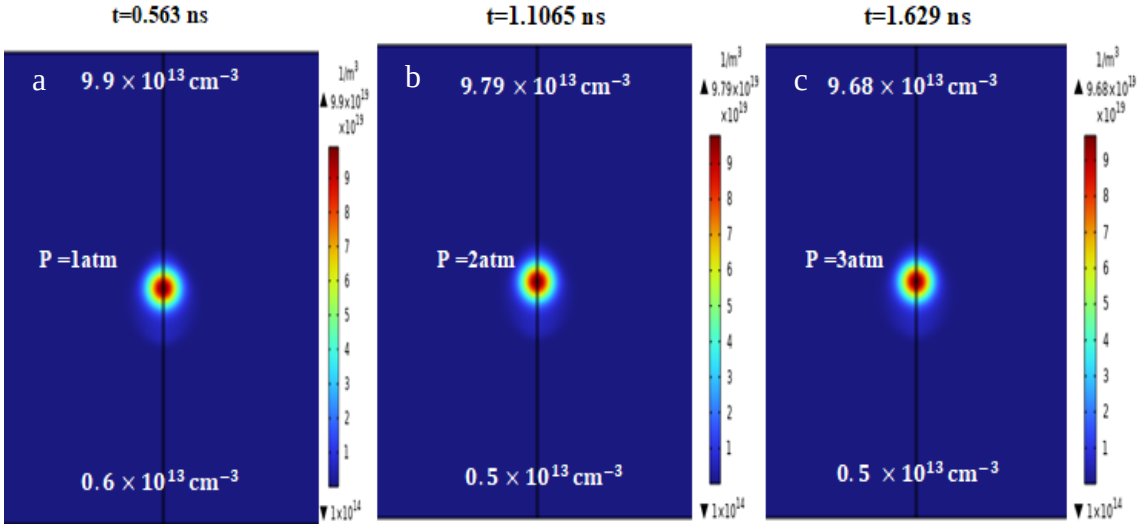

Figure 4: Two-dimensional surface plots of the electron density (the propagation stage) of a double-head streamer discharge extending between Plane-to-Plane electrodes.

Fig. 5 shows the electron density for the interaction stage of the double-head streamer discharge in the air for the different pressure values. It can be seen that the negative streamer reached the anode and interacted with it. For the 1atm pressure, the negative streamer crossed the inter-electrode space of 0.25 cm in 4.504 ns with an electron density of 1.67×10^{14} cm^{-3}, corresponding to an average speed estimated at about 0.56 mm/nm. When the pressure increased to 2atm, the negative streamer crossed the inter-electrode space of 0.25 cm in 9.9585 ns with an electron density of 1.43×10^{14} cm^{-3}, corresponding to an average speed of about 0.35 mm/ns. At 3atm pressure, the negative streamer crossed the inter-electrode space of 0.25 cm in 14.661 ns with an electron density of 1.24×10^{14} cm^{-3}, corresponding to an average speed of about 0.17mm/ns.

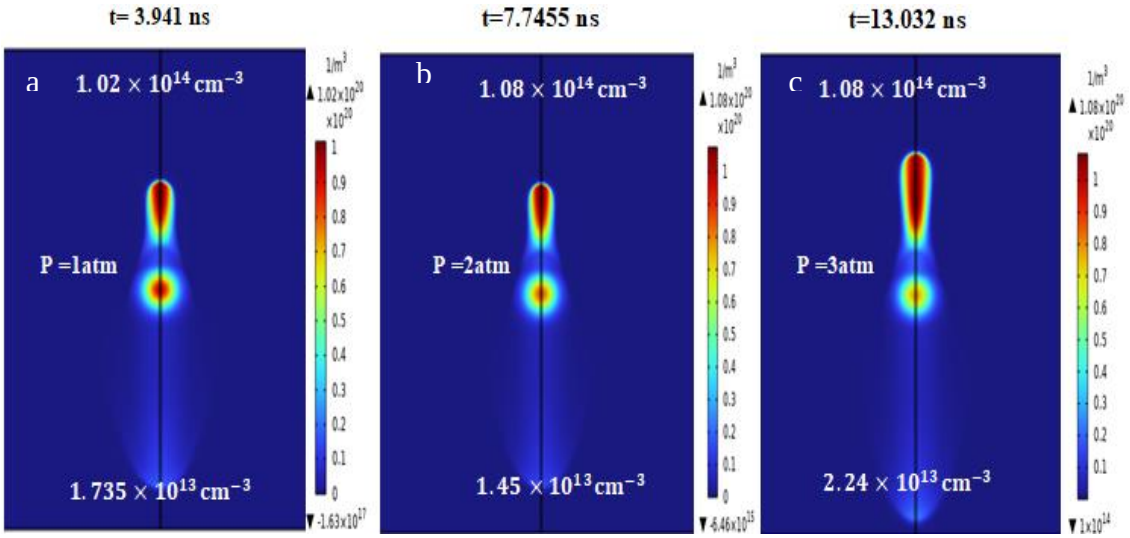

Figure 5: Two-dimensional surface plots of the electron density (the interaction stage) of a double-head streamer discharge extending between Plane-to-Plane electrodes.

Fig. 6 shows the electrons density for the breakdown stage of the double head streamer discharge for different values of pressure. In this stage, the propagation of the cathode-directed streamer is only possible because it is given a high enough background electron density. The breakdown stage has occurred as the enhanced region of the electric field reaches the cathode. The electron density for the positive streamer does not reach the cathode, as 'electrical breakdown' had occurred. For 1atm, the 0.5cm air gap between plane and plane will be broken down after 5.63 ns. The positive streamer crosses the inter-electrode space of 0.244 cm with the electron number density 2.01×10^{14} cm^{-3}, which corresponds to an average speed estimated at about 0.44 mm/ns. For 2atm, the 0.5cm air gap between plane and plane will be broken down after 11.065ns. The positive streamer crosses the inter-electrode space of 0.244 cm with the electron number density 2.69×10^{14} cm^{-3}, which corresponds to an average speed estimated at about 0.22 mm/ns. For 3atm, the 0.5 cm air gap between plane and plane will be broken down after 16.29 ns. The positive streamer crosses the inter-electrode space of 0.244 cm with the electron number density 2.89×10^{14} cm^{-3}, which corresponds to an average speed estimated at about 0.15 mm/ns.

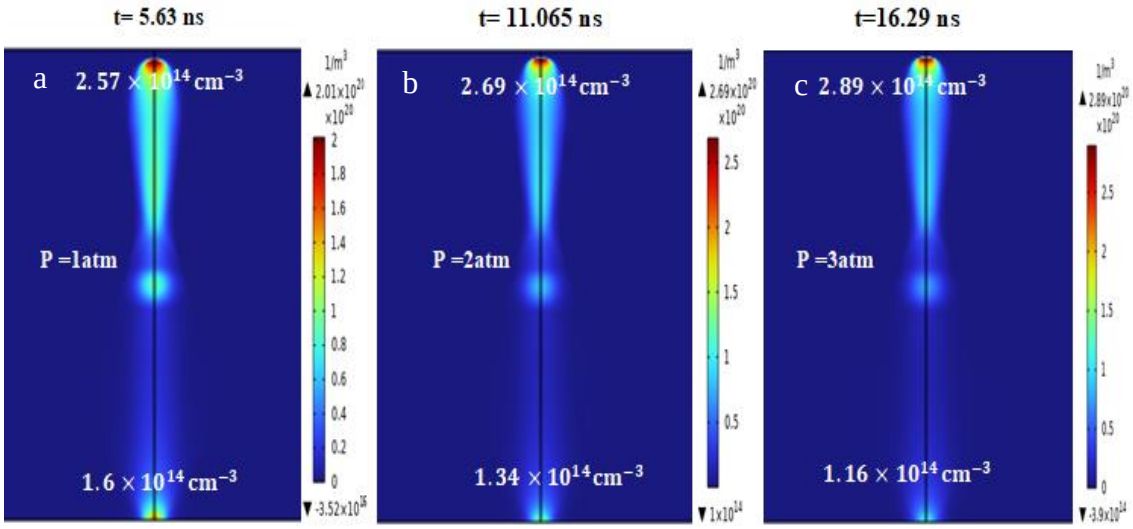

Figure 6: Two-Dimensional surface plots of the electron's density (the breakdown stage) of a double-head streamer discharge extending between Plane-to-Plane electrodes.

3.2. Electric Field Strength

The electric field intensity graphs of the double-head streamer discharge growth under 1, 2 and 3 atm pressures are shown in Fig. 7a–c. Every curve in the diagram illustrates how the electric field intensity changed along the axisymmetric path from the start of the double-head streamer discharge until the breakdown point. This graphic shows how the impact ionization, collision, and drift of charged particles were accelerated during the double-head streamer discharge process as the pressure was increased. The impact ionization enhances the discharge intensity in the head area of the positive and negative streamers. The net space charge also grew, causing the external electric field to shift more noticeably due to the negative and positive space charges. It can be seen that for each pressure value, the electric field in the positive streamer head was higher than that in the negative streamer head, while the electric field in the negative streamer channel was higher than that in the positive streamer channel.

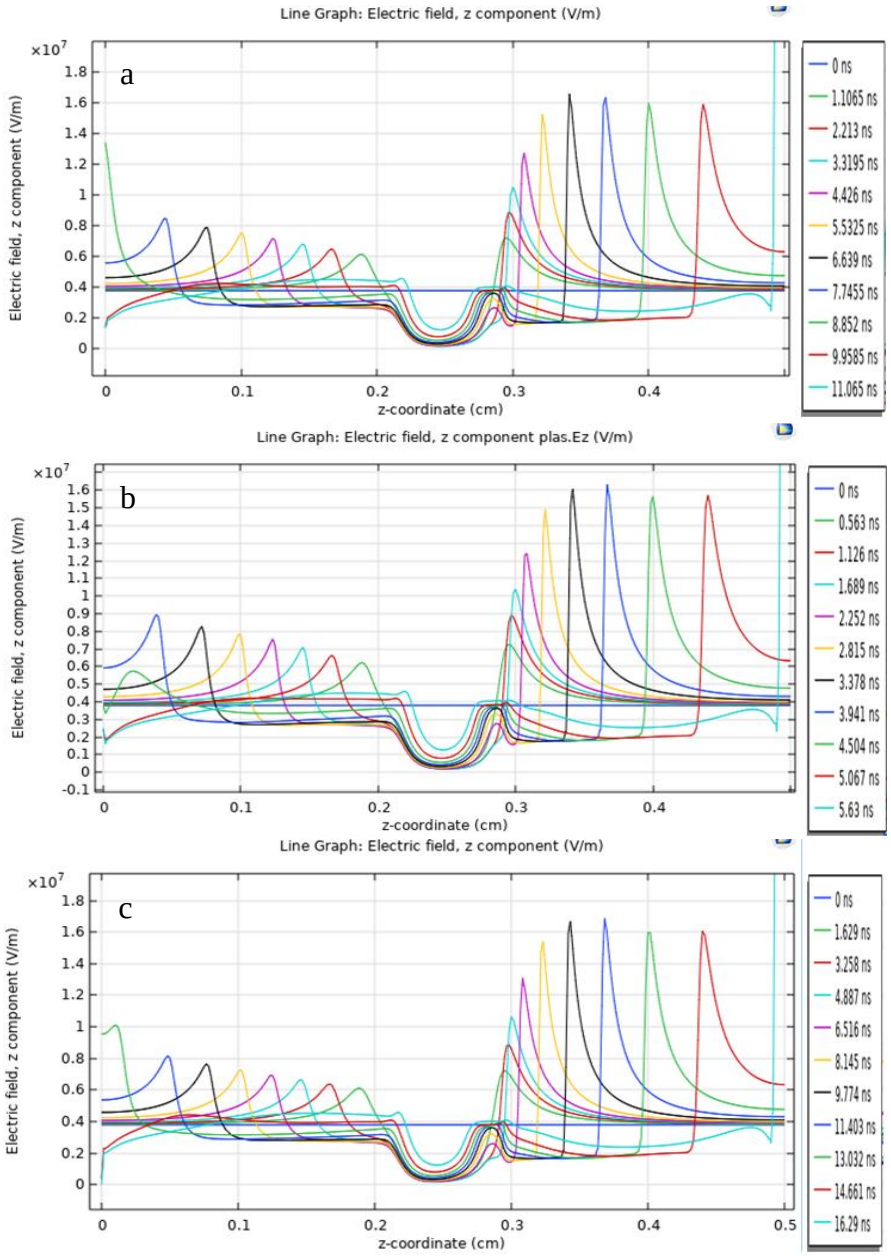

Figure 7: The electric field intensity along the axis for (a) 1atm (b) 2atm and (c) 3atm pressures.

3.3. Space Charge Distribution

One-dimension graphs of the space charge density of the double-head streamer discharge growth at 1, 2 and 3 atm pressures are displayed in Fig. 8. Each curve displays the variation in the space charge density along the axis of symmetry from the start of the double-head streamer discharge to the breakdown point. The positive net charge is greater than the negative net charge. The maximum of the positive net charge density is approximately ten times greater than that of the negative net charge density because of the attaching effect.

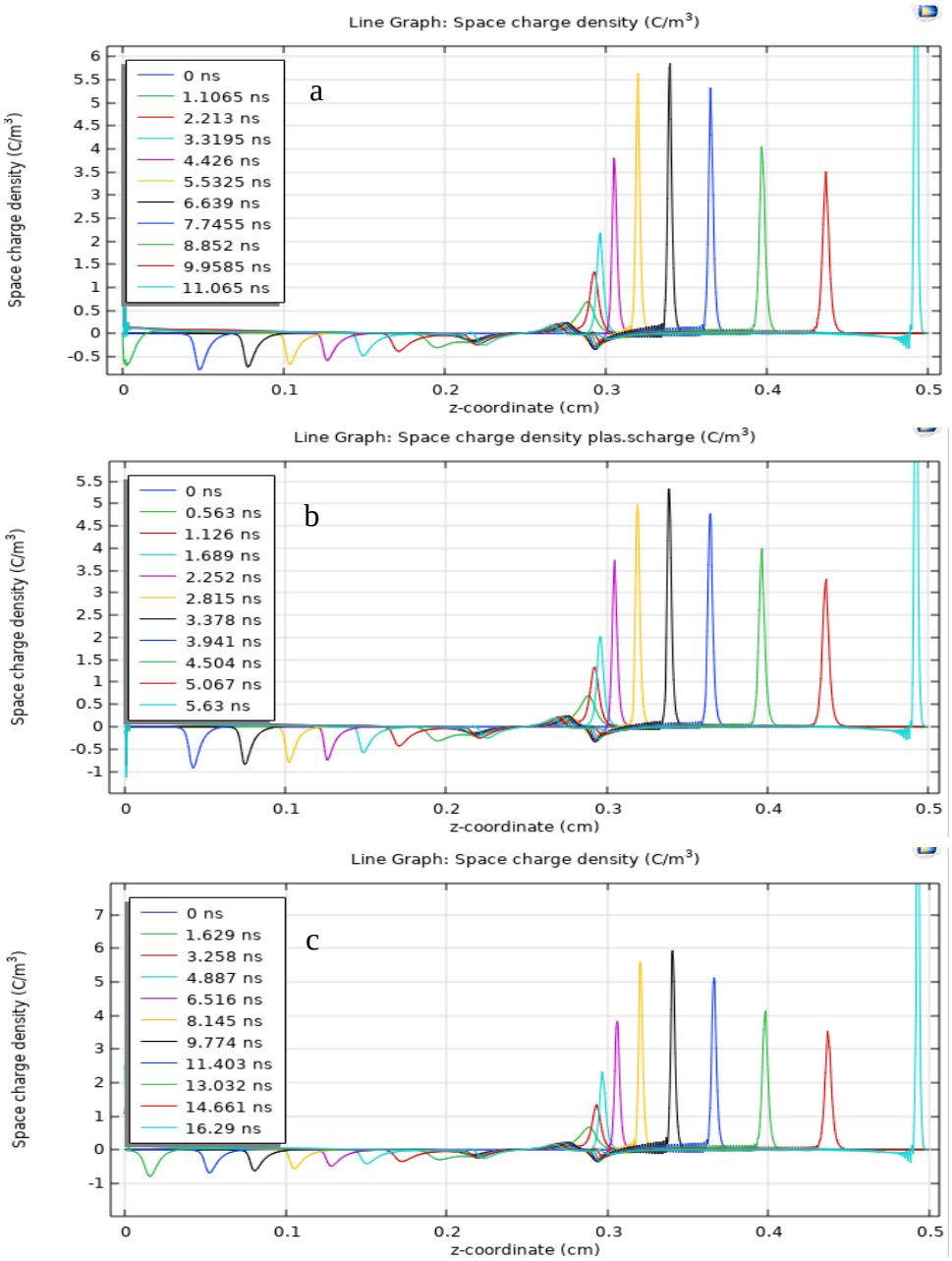

Figure 8: The space charge distribution along the axisymmetric for (a) 1atm (b) 2atm and (c) 3atm pressures.

4. Conclusions

The simulation's results lead us to the following conclusions:

- As air pressure decreases, the double-head streamer discharge develops more quickly.
- For each value of pressure, the electron density of the negative streamer head is smaller than that of the positive streamer head, and the electron concentration decreases with a decrease in air pressure.
- The results indicate that the decrease in pressure has a minimal effect on the electric field. The streamer head's field strength increases with air pressure.

Conflict of interest

Authors declare that they have no conflict of interest.

References

1. T. H. Khalaf and M. F. Abd Alameer, AIP Conference Proceedings (Dubai, United Arab Emirates AIP Publishing, 2021). p. 060009.
2. A. Bourdon, Z. Bonaventura, and S. Celestin, Plas. Sour. Sci. Tech. **19**, 034012 (2010). DOI: 10.1088/0963-0252/19/3/034012.
3. S. Nijdam, J. Teunissen, and U. Ebert, Plas. Sour. Sci. Tech. **29**, 103001 (2020). DOI: 10.1088/1361-6595/abaa05.
4. H. L. Francisco, Ph. D Thesis, Eindhoven University of Technology, 2023.
5. L. Bo, Ph. D Thesis, National University of Singapore, 2020.
6. D. Bouwman, H. Francisco, and U. Ebert, Plas. Sour. Sci. Tech. **32**, 075015 (2023). DOI: 10.1088/1361-6595/ace792.
7. Z. Wang, A. Sun, and J. Teunissen, Plas. Sour. Sci. Tech. **31**, 015012 (2022). DOI: 10.1088/1361-6595/ac417b.
8. A. H. Markosyan, J. Teunissen, S. Dujko, and U. Ebert, Plas. Sour. Sci. Tech. **24**, 065002 (2015). DOI: 10.1088/0963-0252/24/6/065002.
9. C. Montijn, W. Hundsdorfer, and U. Ebert, J. Comput. Phys. **219**, 801 (2006). DOI: 10.1016/j.jcp.2006.04.017.
10. C. Li, U. Ebert, and W. Brok, IEEE Transact. Plas. Sci. **4**, 910 (2008). DOI: 10.1109/TPS.2008.922487.
11. C. Li, U. Ebert, and W. Hundsdorfer, J. Comput. Phys. **231**, 1020 (2012). DOI: 10.1016/j.jcp.2011.07.023.
12. J. Teunissen, Ph.D Thesis, The Dutch Technology Foundation STW, 2015.
13. S. Singh, Ph. D Thesis, Chalmers University of Technology, 2017.
14. G. E. Georghiou, R. Morrow, and A. Metaxas, J. Phys. D Appl. Phys. **33**, 2453 (2000). DOI: 10.1088/0022-3727/33/19/316.
15. M. F. Abdulameer and T. H. Khalaf, Journal of Physics: Conference Series (Athens, Greece IOP Publishing, 2024). p. 012019.
16. G. S. Kadhim and T. H. Khalaf, Iraqi J. Sci. **63**, 2453 (2022). DOI: 10.24996/ijs.2022.63.6.12.
17. H. H. Marza and T. H. Khalaf, Iraqi J. Phys. **20**, 98 (2022). DOI: 10.30723/ijp.v20i3.1017.
18. A. A. Kulikovsky, IEEE Transact. Plas. Sci. **29**, 313 (2001). DOI: 10.1109/27.922740.
19. C. Zhuang and R. Zeng, Communic. Comput. Phys. **15**, 153 (2014). DOI: 10.4208/cicp.210213.300413a.
20. S. Soulie, Ph.D Thesis, Université Grenoble Alpes, 2021.
21. S. Celestin, Ph.D Thesis, Ecole Centrale Paris, 2008.
22. *Negative Streamer in Nitrogen*, COMSOL Multiphysics; https://www.comsol.com/model/negative-streamer-in-nitrogen-44551.
23. W.-G. Min, H.-S. Kim, S.-H. Lee, and S.-Y. Hahn, IEEE Trans. Magnet. **36**, 1280 (2000). DOI: 10.1109/20.877674.
24. L. V. M. Fabris and J. C. C. D. Silva, J. Microw. Optoelect. Electromag. Appl. **21**, 481 (2022). DOI: 10.1590/2179-10742022v21i4263644.
25. W.-G. Min, H.-S. Kim, S.-H. Lee, and S.-Y. Hahn, IEEE Transact. Mag. **37**, 3141 (2001). DOI: 10.1109/20.952562.

26. L. R. Strobel, C. Nguyen, and C. Guerra-Garcia, AIAA SciTech 2022 Forum (USA Massachusetts Institute of Technology, 2021). p. 378.
27. L. R. Strobel, C. Nguyen, and C. Guerra-Garcia, *Multiscale Modeling of Streamers: High-Fidelity Versus Computationally Efficient Methods*, *Aiaa Scitech 2022 Forum*.
28. A. F. Al-Rawaf and T. H. Khalaf, Journal of Physics: Conference Series (Baghdad, Iraq IOP Publishing, 2022). p. 012066.

تحليل محاكاة تفريغ التدفق ثنائي الرأس تحت ضغوط مختلفة

مها فاروق عبد الأمير[1] وثامر حميد خلف[1]
[1] قسم الفيزياء، كلية العلوم، جامعة بغداد، بغداد، العراق

خلاصة

في هذا البحث تم عرض ديناميكيات بدء تفريغ التيار ثنائي الرأس وانتشاره وتفاعله وانهياره في الهواء تحت قيم ضغط مختلفة. تم تحليل ديناميكيات تفريغ التيار ثنائي الرأس داخل تكوين قطب كهربائي من مستوى إلى مستوى. تم ذلك من خلال العديد من الجوانب المقترحة، مثل كثافة الإلكترون والحقل الكهربائي وكثافة الشحنة الفضائية وسرعة انتشار التيار. تعتمد المحاكاة التي أجريت باستخدام "COMSOL Multiphysics" على طريقة العناصر المحدودة وتم تنفيذها باستخدام نموذج السوائل. يصف نموذج السوائل حركة تركيزات الجسيمات باستخدام معادلات التفاضل الجزئي (PDEs) جنبًا إلى جنب مع معادلة بواسون؛ تحدد معادلة بواسون وتركيزات الشحنة توزيع المجال الكهربائي في الفضاء. وفقًا للنتائج، مع زيادة الضغط من (1 و2 و3 ضغط جوي)، زاد وقت تطور التيار من (0.563 إلى 16.29 نانوثانية) بنفس جهد الانهيار 19 كيلو فولت. هذا يعني أن تفريغ التيار ثنائي الرأس تطور بشكل أسرع مع انخفاض الضغط.

الكلمات المفتاحية: تفريغ غاسل، نموذج الموائع، طريقة العناصر المحدودة، فجوة هواء بين مستووين، COMSOL Multiphysics.